



Adsorbents Selection for Caffeine Removal from Green Tea Extract

Dat Quoc Lai^{1,2}, Hien Thi Nguyen^{1,2}, Khanh Quoc Do^{1,*}

¹ Department of Food Technology, Faculty of Chemical Engineering, Ho Chi Minh City University of Technology (HCMUT), 268 Ly Thuong Kiet Street, District 10, Ho Chi Minh City, Vietnam

² Vietnam National University Ho Chi Minh City, Linh Trung Ward, Thu Duc District, Ho Chi Minh City, Vietnam

* Email: dqkhanh.sdh231@hcmut.edu.vn

ARTICLE INFO

Received: 25/01/2026

Accepted: 02/03/2026

Issued date: 30/03/2026

Keywords:

Caffeine

Tea

Separation

Adsorption

Nanotechnology

ABSTRACT

Tea (*Camellia sinensis*) is well known for bioactive metabolites especially polyphenols and caffeine, providing numerous health benefits, but the overconsumption of caffeine causes health risks to vulnerable people. The traditional decaffeination methods are primarily concerning potential chemical residues, the loss of beneficial compounds, the costly and complex processing. This study aims to evaluate an alternative decaffeination method by different adsorbents (Purolite C100, Mixbed and Mordenite Zeolite). In simulated caffeine solutions (400–2000 mg/L), the optimal adsorbent was MOR zeolite, Mixbed and Purolite C100. MOR Zeolite was applied in real green tea extract, yielding a caffeine removal rate of $85.895 \pm 0.03\%$ and adsorption capacity of 10.194 ± 0.004 mg/g, while polyphenol removal rate of $21.079 \pm 0.076\%$ and adsorption capacity of 6.459 ± 0.023 mg/g. The kinetics models of MOR zeolite for caffeine systems were well represented by the pseudo-second-order (PSO) model, while the pseudo-first-order (PFO) model fitted for polyphenol.

Introduction

Tea (*Camellia sinensis*), is one of the popular recipes in Asian countries and now widely used around the world for health benefits of several bioactive compounds such as polyphenols, caffeine, fats, amino acids, flavoring chemicals, vitamins, chlorophyll and other substances. Polyphenols accounts for the majority dry weight of green tea and are reported for positive influence human health [1-5]. Meanwhile, caffeine is one the most popular stimulant and psychoactive substance in the world [6, 7]. Caffeine is well known for its potential to enhance human health [8-10]. However, the overconsumption of caffeine can cause various adverse effects, especially toxicity leading to

potentially life-threatening conditions, ranging from mild discomfort to severe toxicity, including life-threatening complications such as seizures and cardiac arrhythmias [11-13].

Several decaffeination methods have been developed to meet this demand, such as hot water extraction [14], ionic liquid [15-18], supercritical carbon dioxide processing [19-23] and membrane filtration [24-26]. However, the similar disadvantages of current decaffeination methods are the loss or alteration of flavor compounds and overall sensory quality; partial or non-selective removal of bioactive/health-beneficial compounds, energy-intensive or environmentally burdensome processes and technical complexity and strict process control. Adsorption-based techniques

have emerged as one of the most extensively investigated methods for caffeine removal, primarily due to their superior efficiency, ease of operation, and favorable environmental profile. This study experiments 3 distinct classes of commercial adsorbents: Purolite C100, Mixed ion-exchange resins, and MOR zeolite. Purolite C100 is a strong-acid cation-exchange resin (polystyrene-DVB matrix functionalized with sulfonic acid groups). Mixed-bed Indion MB-6SR resins are a combination of strong-acid cation and strong-base anion exchangers. Meanwhile MOR zeolite (Si/Al \approx 10–20) offers a microporous aluminosilicate framework with pore apertures of \approx 6.5–7.0 Å, ideally suited to the molecular dimensions of caffeine (\approx 6.8 \times 5.2 Å). Its high hydrophobicity/hydrophilicity balance and possesses a distinct two-dimensional pore system composed of large 12-membered ring (12-MR) channels (6.5 \times 7.0 Å) interconnected with smaller 8-membered ring (8-MR) channels (2.6 \times 5.7 Å). The study aims to find the most effective adsorbent for caffeine removal with the ultimate goal of evaluating its adsorption behaviors in green tea extract.

Experimental

Chemical

The MOR zeolite was synthesized by D.Lai [27] according to the technical notes provided by M.L. Mignoni [28]. The Purolite C100 (Cation Na⁺) was bought from Ecomax Water, which has polymer structure with divinylbenzene cross-linked polystyrene gel, acid sulfonic -SO₃⁻ functional group and Na⁺ ionic form.

The Mixed (Indion MB-6SR) was from India, which has polystyrene configuration linked with 2 groups primary sulfonic acid and trimethylamine, -SO₃⁻ (sulfonic acid) và -NR₃⁺ (trimethylamine) functional groups and H⁺/OH⁻ ionic form.

Green tea leaves (*C. sinensis*) were sourced from a commercial plantation in Lam Dong Province, Vietnam. After being washed, the green tea leaves were removed from the hard branches, brown leaves, and wilted leaves, and steamed at 121°C for 5 minutes to inactivate the enzyme [29]. Then, the tea was ground by a food blender to recover the soluble substances, mixing with deionized water, the ratio of tea and water was 1: 3 (w/v) [30, 31]. The slurry was put into a filter cloth, and the press is used to squeeze out the residue to collect the extract. The extracted extract was roughly filtered using a filter bag with a pore size of 100 microns and 25 microns. After dry filtration, the extract continued to be filtered through 2 polypropylene filter

columns with a membrane pore size of 5 microns and 1 micron. The extract was then stored at 4°C for following experiments.

Other chemicals used in this study were of analytical grade and supplied by Sigma-Aldrich.

Methods

Green tea extract was assayed for total soluble solid content, total polyphenol, caffeine, pH, and antioxidant activity according to FRAP.

The total soluble solid content of the tea extract was determined using a refractometer (Model 300010, Sper Scientific) at room temperature. Results were expressed as degrees Brix (°Brix).

Total polyphenol content was measured by ultraviolet-visible (UV/Vis) spectrophotometry using Folin-Ciocalteu assay at 765nm wavelength on UV-VIS spectrophotometer UV1100 in three replicates according to standard ISO 14502-1 [30].

Caffeine content was extracted from the infusion using chloroform and determined by UV-Vis spectrophotometry, with absorbance measured at 274 nm in three replicates [31].

Antioxidant activity according to DPPH: The antioxidant activity of the extracts was evaluated on the basis of their ability to scavenge free radicals. This method is based on the ability of antioxidants to convert the stable free radical DPPH into its nonradical form, resulting in a color change of the solution from purple to yellow. The absorbance of the resulting mixture was recorded using UV-Vis spectrophotometry at 515 nm [30].

Antioxidant activity according to FRAP, the method operates on the principle that antioxidants convert the ferric-tripyridyl-triazine complex (Fe³⁺-TPTZ) into a blue ferrous form, which is measured by absorbance at 595 nm [30].

Caffeine Adsorption Behavior in a Simulated Green Tea Extract Solution of Different Resins

Sample preparation

The simulation solution was prepared by dissolving 99% crystalline anhydrous caffeine in distilled water at concentrations of 400 mg/L, 800 mg/L, 1200 mg/L, 1600 mg/L and 2000 mg/L respectively. The purpose of using this solution is to remove interfering factors (such as complex systems between caffeine and polyphenols, minerals, proteins, etc.), factors that cause fouling of resin particles such as suspended particles in untreated natural tea water that will affect the ion exchange process.

Effects of pH

Preparation: A simulated green tea solution with an initial caffeine concentration of 1600mg/L was prepared and the initial pH was modified to pH = 2, 3, 4 and 5 using a 5% citric acid solution (pH = 1.81 ± 0.02). The ratio of solution : adsorbent = 10 : 1 (v/w).

Procedure: 10g of each adsorbent was added into a 100mL Erlenmeyer with 100ml of each simulated solution, sealed and stirred at the speed of 200 r/min, at room temperature 30 ± 1°C. Then 1 mL aliquots were taken every hour for analyzing residual caffeine concentration until equilibrium.

Adsorption capacity: reflected the amount of substance adsorbed per unit dry mass of the adsorbent – mg of substance/g of adsorbent (mg/g), at a given time Q_t and at equilibrium Q_e were determined by equation (3) and (4)

$$Q_t = \frac{(C_0 - C_t) \cdot V}{m} \quad (1)$$

$$Q_e = \frac{(C_0 - C_e) \cdot V}{m} \quad (2)$$

where: C_0 – the initial adsorbate concentration (mg/L), C_t – adsorbate concentration at a given time (mg/L), C_e – equilibrium adsorbate concentration (mg/L), V – the volume of adsorbate solution (L), m – mass of the adsorbent (g).

Removal efficiency: reflected the ratio of substance adsorbed by adsorbents compared to the initial concentration in the solution was determined by equation (3)

$$H = \frac{(C_0 - C_e) \cdot 100\%}{C_0} \quad (3)$$

where C_0 and C_e are the concentrations at the initial stage and at equilibrium, respectively.

Kinetic model of caffeine adsorption

Preparation: A simulated green tea solution with an initial caffeine concentration of 1600mg/L was prepared and the initial pH was modified to pH = 2 using a 5% citric acid solution (pH = 1.81 ± 0.02). The ratio of solution : adsorbent = 10 : 1 (v/w).

Procedure: 10g of each adsorbent was added into a 100mL Erlenmeyer with 100ml of each simulated solution, sealed and stirred at the speed of 200 r/min, at room temperature 30 ± 1°C for 4 hours and the solution was collected for measuring residual caffeine concentration every 30 minutes. The kinetic data for caffeine adsorption were fitted to the pseudo-first-order (PFO) and pseudo-second-order (PSO) models.

Adsorption kinetics model

The adsorption kinetic model explains the rate and mechanism of adsorption of contaminants onto the

material surface, allowing prediction of treatment efficiency, optimization of operating conditions and design of adsorbent materials. The kinetics of the adsorption process is studied by two kinetic models: pseudo-first-order (PFO) (4) and pseudo-second-order (PSO) (5) [32, 33]

$$Q_t = Q_e (1 - e^{-k_1 t}) \quad (4)$$

$$\frac{t}{Q_t} = \frac{1}{k_2 \cdot Q_e^2} + \frac{t}{Q_e} \quad (5)$$

where Q_e - the adsorption capacity at equilibrium (mg/g); Q_t - the adsorption capacity at time t (mg/g); t - the adsorption time (min); k_1 and k_2 - the first-order (1/min) and second-order (g/mg.min) rate constants, respectively.

Isotherm model of caffeine adsorption

Preparation: The simulated solutions with caffeine concentrations of 400 mg/L, 800 mg/L, 1200 mg/L, 1600 mg/L and 2000 mg/L were adjusted to pH 2 with 5% citric acid solution (pH 1.81 ± 0.02). The ratio of solution : adsorbent = 10 : 1 (v/w).

Procedure: 10g of each adsorbent was added into a 100mL Erlenmeyer flask with 100ml of each simulated solution, sealed and stirred at the speed of 200 r/min, at room temperature 30 ± 1 °C. The mixing time was 4 hours for Purolite C100 and MOR zeolite, 7 hours for Mixbed, then the solution was settled and collected for analyzing residual caffeine concentration. The data for caffeine adsorption were fitted to the Langmuir and Freundlich models.

Langmuir isotherm model [34]

$$Q_e = \frac{Q_{max} \cdot K_L \cdot C_e}{1 + K_L \cdot C_e} \quad (5)$$

Where K_L - equilibrium (affinity) constant, Q_e - equilibrium adsorption capacity (mg/g), Q_{max} - maximum adsorption capacity on a monolayer (mg/g) and C_e - equilibrium adsorbate concentration (mg/L)

Another index that can evaluate the compatibility of the Langmuir model is the dimensionless separation constant R_L

$$R_L = \frac{1}{1 + \frac{C_0}{K_L}} \quad (6)$$

If $R_L = 0$ – the model is irreversible, $0 < R_L < 1$ – the model is favorable adsorption, $R_L > 1$ – the model is linear and $R_L > 1$ – the model is unfavorable

Freundlich isotherm model [35]:

$$Q_e = K_F \cdot C_e^{\frac{1}{n}} \quad (7)$$

where both K_F and $\frac{1}{n}$ is Freundlich constant. If $\frac{1}{n} = 0$ – the model is irreversible, $0 < \frac{1}{n} < 1$ – the model is

favorable adsorption, $\frac{1}{n} = 1$ – the model is linear and $\frac{1}{n} > 1$ – the model is unfavorable.

Caffeine and polyphenol adsorption behavior of MOR zeolite in green tea extract

Preparation: The green tea extract was adjusted to pH=2 by a citric acid 5% solution (pH = 1.81 ± 0.02). The ratio of solution : adsorbent = 10 : 1 (v/w).

Procedure: 10g of MOR zeolite was added into a 100mL Erlenmeyer flask with 100ml of green tea extract, sealed and stirred at the speed of 200 r/min, at room temperature 30 ± 1 °C, then the solution was collected every 30 minutes for analyzing residual caffeine and polyphenol concentration until equilibrium and the kinetic data for caffeine adsorption were fitted to the pseudo-first-order (PFO) and pseudo-second-order (PSO) models.

Statistical analysis

Each experiment was replicated three times ($n = 3$), with results that are presented as the mean \pm standard deviation (SD). Statistical analysis was carried out using one-way ANOVA followed by Tukey–Kramer HSD post hoc tests using IBM SPSS Statistics 20. For all tests, a p value of less than 0.05 was considered to indicate a statistically significant difference.

Results and discussion

Components analysis of green tea extract

The results showed in Table 1 that the total soluble solids content was 2.46 Brix, which showed that in 1L of green tea extract there were 2.46g of soluble solids. The pH of the tea extract was 4.63 ± 0.057 , slightly acidic, which is similar to polyphenols and caffeine and can be explained by the large influence of the pH of the water used for processing during the process.[36, 37].

Regarding the chemical components, total polyphenol content accounted for the largest component with 124.57 ± 0.964 mg/g, and the total caffeine content was 48.246 ± 0.139 mg/g. Comparing to the previous study by Gonçalves Bortolini et al. (2021), the polyphenol content was in the range of 12.36 – 252.65 mg/g while the caffeine content was higher than the reported data, 2.64 – 42.20 mg/g. Besides that, the total aluminum content Al in green tea extract was 1.642 ± 0.001 mg/g, consistent with the surveyed content range of 0.272 - 3.26 mg/g in previous studies [38, 39]. This can be explained by the difference in origin, climate conditions, growth of different types of

tea or maybe due to the conditions of the water source used in the process of processing the tea extract [37, 40]. The antioxidant activity by FRAP method, Trolox concentration ($\mu\text{mol TE/g}$) was used to evaluate antioxidant activity, reaching a value of 171.028 ± 0.245 $\mu\text{mol TE/g}$, which was fitted to the previous study with the antioxidant activity in the range of 164 - 175 $\mu\text{mol TE/g}$ [41]

Table 1: Initial composition of green tea extract

| | Unit | Value |
|----------------------|---------------------------------------|---------------------|
| Total soluble solid | Brix | 2.46 ± 0.052 |
| Total polyphenol | mg/g soluble solid | 124.57 ± 0.964 |
| Total caffeine | mg/g soluble solid | 48.246 ± 0.139 |
| pH | - | 4.630 ± 0.057 |
| Antioxidant activity | Trolox concentration | 171.028 ± 0.245 |
| FRAP | ($\mu\text{mol TE/g}$ soluble solid) | |

Caffeine adsorption behavior of different adsorbents in simulated solution

Optimal conditions

According to the results in caffeine removal efficiency, pH showed a significant impact on the adsorbents. Both Mixbed and MOR zeolite had the highest removal efficiency, $88.440 \pm 0.01\%$ and $89.089 \pm 0.005\%$, at pH=2 and decrease gradually as pH increase. While the adsorption capacity and removal efficiency of Purolite C100 increase as pH increase from 2 and reached the maximum at pH = 3, 5.205 ± 0.002 mg/g and $32.534 \pm 0.010\%$ then decrease gradually from pH = 4 and 5. Moreover, Mixbed and MOR zeolite brought higher adsorption results, about 2-2.5 times, than Purolite C100. The decaffeination process of these materials occurs via adsorption, influenced by both the pKa value of caffeine (5.3 – 14) and the pH of the solution (pH = 2 – 3). When the pKa of caffeine is greater than the solution pH, the caffeine is protonated, becoming positively charged at the N8/N9, O11, and O12 groups [42, 43]. Caffeine has a high dipole moment, which increases with the polarity of the environment. This causes the positive charges on the caffeine groups to electrostatically interact with the negatively charged polar functional groups on the material surface, resulting in caffeine being retained on the adsorbent materials and removed from the solution [40]. Among the materials, mixed bed particles carry a negative charge due to the active SO_3^- group and OH^- ions, which have the ability to interact electrostatically with a larger number of groups; MOR zeolites have a negatively charged aluminosilicate

framework (the extended isomorphic substitution of Si^{4+} by Al^{3+} in the tetrahedron, leading to a negative charge in the surrounding O-) and both yield high decaffeination results [44-47]. Meanwhile, cation exchange resins (Purolite C100) also have SO_3^- active groups, but the ions are in the form of Na^+ , which limits the decaffeination process (due to fewer electrostatically interacting groups) and results in lower efficiency under the same conditions. Didinedin's research stated that pH had greatly influences on caffeine adsorption and highly acidic solutions exhibited enhanced caffeine removal efficiency [39]. Or in another study of Bachmann et al. regarding the topic of caffeine removal by adsorption, studies have been compiled showing similar results: at lower pH, the caffeine adsorption capacity is higher [48]. The optimum pH depends on the surface charge of the adsorbent and the degree of ionization of the adsorbed molecules, so different pH values were optimal when evaluating different adsorbents used for caffeine removal [49]. From an application perspective, although pH = 2 is more acidic than typical beverage conditions and uncommon in industrial processes, particularly in extraction, purification, and food processing systems. Moreover, the adsorption step can be followed by a neutralization process to restore the pH of the final product. It is also important to note that the relatively mild operating temperature ($30 \pm 1^\circ\text{C}$) and controlled contact time help minimize the degradation of sensitive compounds, as reflected by the moderate loss of polyphenols observed in this study. Consequently, the pH = 2 was selected for other experiments due to high decaffeination efficacy in this study. Future researches should focus on optimizing the process under milder pH conditions while maintaining acceptable selectivity-performance trade-offs.

With the increasing of caffeine concentration from 400 to 2000 mg/L, the removal efficiency of all adsorbents decreased slightly when caffeine concentration increased, $37.022 \pm 0.076\%$ to $22.382 \pm 0.003\%$ for Purolite C100, $88.734 \pm 0.063\%$ to $88.102 \pm 0.006\%$ for Mixbed, $89.204 \pm 0.105\%$ to $88.901 \pm 0.004\%$ for MOR zeolite. This phenomenon can explain that initially the active sites of the adsorbent were still many, when increasing the caffeine concentration of the simulated solution, the larger the caffeine, the greater the adsorption force, this force was created from the concentration gradient, caffeine moved quickly towards the surface of the resin and the activity increased the interaction of caffeine with the active sites on the adsorbents [49]. During adsorption, caffeine molecules must first overcome the stagnant

liquid film surrounding each adsorbent – a process governed by Fick's first law. The flux, J , is given by $J = k(C_0 - C_s)$, where k is the mass transfer coefficient, C_0 is the bulk concentration, and C_s is the surface concentration. When C_0 increases, $(C_0 - C_s)$ grows, so more molecules penetrate the film per unit time [49-52]. At low initial concentrations, the number of active sites were abundant relative to the number of caffeine molecules, leading to a high removal percentage. Conversely, at higher concentrations, the fixed number of active sites on the adsorbents became increasingly saturated, leaving a larger fraction of caffeine molecules unabsorbed in the solution and thus resulting in a lower overall removal efficiency.

Adsorption kinetics

Adsorption kinetic studies were conducted to investigate the rate of caffeine uptake by Purolite C100, Mixbed and MOR Zeolite to elucidate the rate-controlling mechanism. To elucidate the adsorption mechanism, the kinetic data were analyzed using pseudo-first-order and pseudo-second-order models, with the corresponding parameters presented **Table 2**, the pseudo-second-order showed the best describe for Mixbed and MOR zeolite adsorbents due to higher coefficient of correlation and the consistency between its theoretical and experimental adsorption capacities and for Purolite C100 with higher coefficient of correlation but the consistency had larger difference than the pseudo-first-order. Therefore, all adsorbents well fitted the pseudo-second-order (PSO). The applicability of the pseudo-second-order model suggests that the rate-limiting step is the surface adsorption, where the removal from a solution is due to physicochemical interactions between the two phases [53]. Thereby, pseudo-second-order shows that the adsorbents share the same mechanism of chemical adsorption, rather than physical adsorption [54, 55]. The same results were obtained by several previous studies, the caffeine adsorption of adsorbents followed the pseudo-second-order [42, 48].

Adsorption isotherms

Adsorption isotherms describe the distribution of adsorbate molecules on the adsorbent surface, thereby enabling determination of the adsorption mechanism under equilibrium conditions at a fixed temperature. In this work, the equilibrium data for caffeine adsorption onto Purolite C100, Mixbed and MOR Zeolite were obtained at room temperature by measuring the equilibrium capacity (Q_e) at various equilibrium concentrations (C_e). To analyze these data, two well-

established isotherm models were employed: the Freundlich model, and the Langmuir model. Based on the data of Table 2, the Langmuir model demonstrates a better fit than the Freundlich model. The assumption of Langmuir model states that the surface of the adsorbent is homogeneous in energy, the adsorbed molecules form a monolayer on the solid phase surface. Besides that, the Freundlich exponent, $1/n$, also known as the heterogeneity factor, is a crucial parameter that provides insight into the intensity of the adsorption and the heterogeneity of the active site.

The magnitude of the $1/n$ value indicates the favorability of the adsorption process. A value in the range of $0 < 1/n < 1$ signifies favorable adsorption on a heterogeneous surface, where high-energy sites are occupied first, followed by lower-energy sites. A value of $1/n > 1$ would suggest cooperative adsorption. In this study, the calculated values of $1/n$ of all 3 adsorbents were larger than 1, it was confirmed that the adsorption of caffeine onto the Purolite C100, Mixedbed and MOR zeolite were not fitted.

Table 2. Adsorption kinetic and adsorption isotherms parameters of Purolite C100, Mixedbed and MOR zeolite adsorbents in simulated solution at room temperature

| Adsorption kinetics | Pseudo-first-order (PFO) | | | Pseudo-second-order (PSO) | | | Q_e exp (mg/g) |
|----------------------|--------------------------|------------------|--------|---------------------------|---------------------|--------|------------------------|
| | Q_e (mg/g) | k_1 (1/min) | R^2 | Q_e (mg/g) | k_2 (g/mg/min) | R^2 | |
| Purolite C100 | 8.9 | 0.003 | 0.987 | 19.467 | 0.001 | 0.9945 | 4.406 |
| Mixedbed | 10.486 | 0.009 | 0.9596 | 17.252 | 0.006 | 0.9848 | 14.150 |
| MOR zeolite | 10.673 | 0.021 | 0.9497 | 16.357 | 0.001 | 0.9924 | 14.254 |
| Adsorption isotherms | Langmuir | | | Freundlich | | | |
| | K_L | Q_{max} | R^2 | K_F | $1/n$ | R^2 | |
| Purolite C100 | 0.059 | 7.391 | 0.9745 | 127.85 | 1.541 | 0.9629 | |
| Mixedbed | 19.146 | 238.095 | 0.9401 | 12.031 | 1.035 | 0.9997 | |
| MOR zeolite | 36.444 | 434.783 | 0.9532 | 11.706 | 1.02 | 0.9999 | |

Caffeine and polyphenol adsorption behavior in green tea extract

MOR zeolite was selected as the most effective adsorbent for decaffeination. Based on Fig 1, MOR zeolite's caffeine adsorption behavior differed significantly between green tea extract and simulated solution, primarily due to the complex, multi-component nature of the extract, which contains a high concentration of polar compounds, and the interference from competing ions and organic molecules. The MOR zeolite's caffeine adsorption capacity in green tea extract increased gradually, reaching equilibrium after 240 minutes with 10.194 ± 0.004 mg/g, which was lower than in the simulated solution of 17.780 ± 0.001 mg/g. Besides caffeine, a reduction in polyphenol content was also noted during the process. Similarly, the MOR zeolite's polyphenol adsorption capacity also gradually increased with equilibrium at 6.459 ± 0.023 mg/g.

The adsorption selectivity coefficient is an important parameter to evaluate an adsorbent's ability to preferentially adsorb one substance over another when both are present in the system. It is calculated according to the equation

$$K_{Caffeine/Polyphenol} = \frac{Q_e(Caffeine)}{Q_e(Polyphenol)} \times \frac{C_e(Polyphenol)}{C_e(Caffeine)}$$

Here, $C_{e(caffeine)}$ and $C_{e(polyphenol)}$ (mg/L) are the equilibrium concentrations of caffeine and polyphenol in the solutions, respectively; and $Q_{e(caffeine)}$ and $Q_{e(polyphenol)}$ (mg/g) are the equilibrium caffeine and polyphenol adsorption capacity, respectively [56]. This coefficient greater than 1 indicates preferential adsorption of caffeine over polyphenol, while values less than 1 suggest the opposite selectivity. The adsorption selectivity coefficient of caffeine versus total polyphenol was approximately 22.8, which represents exceptionally high selectivity for caffeine separation from polyphenolic compounds. A similar result was calculated to indicate preferential adsorption of caffeine over polyphenol showed the result of 22.5 using polyvinylpyrrolidone (PVPDF) for caffeine-catechin separation [33]. For our specific objective of caffeine extraction from tea extracts, our material's selectivity coefficient of 22.8 (favoring caffeine adsorption) is particularly advantageous, being not only higher in magnitude than both literature examples but also sufficient for removing caffeine from green tea extract. The selective adsorption of caffeine was

explained in a research article of D.Lai [27], containing MOR zeolite's material and surface analysis. Due to the reported results that crystal structure of MOR zeolites is such that the pores are spread throughout the crystal, allowing them to separate molecules with size differences as small as 1Å, and zeolites are size-selective adsorbents [57]. This property reinforces their name as molecular sieves, which are widely used for separation of components based on size exclusion [58]. MOR zeolite possesses a distinct two-dimensional pore system consisting of large (6.5 × 7.0 Å) 12-membered ring (12-MR) channels connected to smaller (2.6 × 5.7 Å) 8-membered ring (8-MR) channels [59, 60]. Meanwhile, caffeine is a small molecule, measuring approximately 0.78 nm in length, 0.61 nm in width, and 0.21 nm in height, making it the ideal size to be retained in the pores of zeolite [61]. In contrast, epicatechin—a relatively simple catechin and the dominant polyphenol in green tea extract—has a more complex molecular structure, characterized by two aromatic rings and five hydroxyl groups [62]. This allowed MOR zeolite to adsorb caffeine selectively and ensure minimal loss of polyphenols. However, there was still a certain number of polyphenols adsorbed but quite small for MOR zeolite due to the small size and the ability to access the pores in the structure of MOR zeolite [27]. The previous research of Damjanović, L., et al. also showed that the adsorption of polyphenol was based on molecular size hypothesis, polyphenol could enter pores and bonded with zeolites through surface active sites [57]. The same results was reported in a research of N. Jiang et al., in which phenol could be adsorbed by zeolites but only revealed from the low adsorption capacity [63]. In addition, Nedić Vasiljević et al. studied that polyphenol created bonds with zeolite bonded through ferulic acid interaction with the functional groups such as -COOH, -CH₃ and aromatic, which are relatively weaker and more surface-limited compared to the adsorption of caffeine [64].

Moreover, the MOR zeolite adsorbent demonstrated a notable performance achieving 85.895 ± 0.03% caffeine removal rate in green tea extract which was also lower than in simulated solution of 89.089 ± 0.006%, while preserving a majority of polyphenols with a loss of only 21.079 ± 0.076%. In fact that there was a quantity of soluble solids in green tea extract solution that form a "cake layer" on the surface of MOR zeolite, increasing the diffusion path length and reducing the accessibility to the pores [50]. When caffeine was adsorbed on real liquids, the results were always lower due to competition in the adsorption process and fouling phenomenon, the "cake layer"

formed on the surface of the adsorbent material [42]. In fact, zeolites are size-selective adsorbents: molecules which are to be adsorbed should be smaller than the pore size of the adsorbent, pollutant molecules with sizes larger than the pore opening of the zeolites can only be adsorbed on the external surface of the zeolite leading to covering, blocking and hindering caffeine from contacting the pores, and in this case adsorption efficiency was decreased [57].

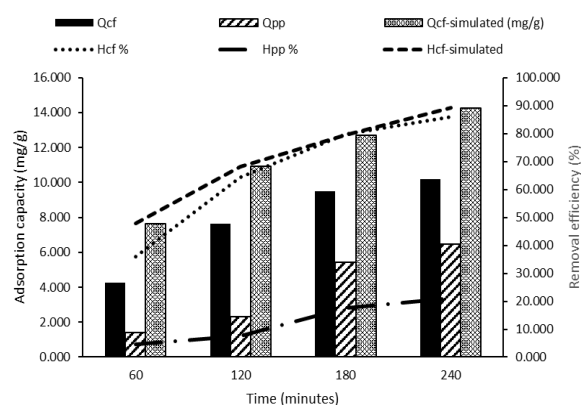


Fig 1: Caffeine and Polyphenol adsorption capacity and removal efficiency on MOR Zeolite as a function of time in green tea extract

The kinetic analysis was then extended to the green tea extract to assess the impact of the complex matrix on the adsorption process. The same PFO and PSO models were employed to allow for a direct comparison with the single-component system previously studied. The R^2 of pseudo-second-order was higher than that of pseudo-first-order (0.9741 > 0.9319) and the Q_e value of pseudo-second-order is closer to the experimental Q_{exp} value. This showed that the caffeine adsorption of MOR zeolite is consistent with the pseudo-second-order (PSO) adsorption kinetic model. The adsorption of caffeine by zeolite takes place through the encapsulation process which was host-guest interaction (established between the functional groups of caffeine with the zeolite silanol groups) and parallel diffusion within the particles of caffeine molecules in the mesopores on the outer surface of the mineral particles [54]. The caffeine adsorption showed that the process fitted the pseudo-second-order adsorption kinetic model and Langmuir isotherm model in most of the reports that were done [42, 48]. Besides that, for polyphenol, the results showed that the R^2 of pseudo-first-order (PFO) was higher with 0.997 while that of pseudo-second-order (PSO) was only 0.9412 and the estimated Q_e value of PFO was also closer to the experimental Q_e . It can be

concluded that the MOR zeolite adsorption of polyphenol was consistent with the pseudo-first-order (PFO) adsorption kinetic model, following physisorption through hydrogen, dipole, ionic bonds... [64]. Compared to a previous study of D.Lai [27], there was a difference in kinetic modeling can be attributed to the dominant rate-controlling mechanism, in which the adsorption process was well described by the pseudo-first-order (PFO) model, suggesting that the diffusion and physisorption. Meanwhile, in this research, the presence of coexisting soluble compounds and fouling phenomena likely increased mass transfer resistance and limited pore accessibility. As a result, the adsorption process became more dependent on surface interactions and intraparticle diffusion, leading to a better fit with the pseudo-second-order (PSO) model. Moreover, this difference may also arise from differences in raw materials, processing conditions, and pretreatment steps. Variations in tea composition and extraction procedures can significantly affect the concentration and nature of coexisting soluble compounds, thereby influencing fouling behavior and competitive adsorption. Furthermore, differences in zeolite synthesis and physicochemical properties (e.g., Si/Al ratio, crystal size, and external surface area) may alter pore accessibility and diffusion pathways. These factors collectively affect the rate-controlling step of the adsorption process, leading to different kinetic model fittings.

The regeneration of adsorbents is a critical factor in evaluating the practical applicability of adsorption systems. In this case, the caffeine removal using mordenite (MOR) zeolite, the ability to restore adsorption capacity after saturation directly influences both economic feasibility and environmental sustainability. Although this study primarily focuses on adsorption performance, future work will systematically evaluate regeneration efficiency and adsorption-desorption cycles to assess durability and performance retention.

Conclusion

This study successfully demonstrated the practical application of the decaffeination method by adsorption in green tea extract. All the adsorbents showed the capability of removing caffeine at the optimal conditions in simulated solutions, in which MOR zeolite removed the most of caffeine, then Mixbed and Purolite C100. From the experiments in simulated system, MOR zeolite was chosen as the optimal adsorbent and it was applied in green tea extract to

evaluate. In green tea extract at the optimal conditions, pH=2, ratio of solution : adsorbent = 10 : 1 (v/w), 4 hours and $30 \pm 1^\circ\text{C}$, MOR zeolite was reported with caffeine removal rate of $85.895 \pm 0.03\%$ while polyphenol loss rate only $21.079 \pm 0.076\%$. Kinetic studies revealed that caffeine adsorption in both simulated solutions and green tea extract well fitted the PSO model, whereas polyphenol adsorption process of MOR zeolite aligned the PFO model, indicating different adsorption behaviors between target and coexisting compounds.

Importantly, the selective adsorption of caffeine by MOR zeolite can be strongly attributed to the geometric effects inherent to its microporous structure. The pore dimensions of MOR zeolite are comparable to the caffeine's molecular size, allowing caffeine to effectively diffuse into the channels and bond with active sites. In contrast, polyphenol are larger and mostly blocked from entering the micropores, leading to the external surface adsorption, which is less favorable and more reversible. This molecular sieving effect not only enhances caffeine selectivity but also helps preserve valuable bioactive compounds in green tea extract.

The results indicate that the potential application of the adsorption method in producing decaffeinated tea extract with all 3 different commercial adsorbents performed the capability of removing caffeine in simulated systems and MOR zeolite was the most effective. In real green tea extract, MOR zeolite exhibited a selective adsorption capacity for caffeine compared to polyphenols, a strong advantage compared to current applied methods. To enhance the effectiveness and practical applicability of this approach, future research should prioritize the assessing the effects of the adsorption process on other key tea constituents (e.g., amino acids and soluble sugars), optimizing the synthesis parameters of the adsorbent to better utilize locally available raw materials while increasing its specific surface area for greater adsorption efficiency, and examining the desorption characteristics and regeneration potential of the zeolite material.

Acknowledgments

Funding for this study was provided by Vietnam National University HoChiMinh City (VNU-HCM) under grant number DN2022-20-01/HĐ-KHCN. We are grateful to Ho Chi Minh University of Technology (HCMUT), VNU-HCM, for the use of their facilities and for supporting our research activities.

References

1. A. Rana, M. Samtiya, T. Dhewa, V. Mishra, S.S. Al-Amiery, *J. Food Biochem.*, 46(10) (2022) e14264. <https://doi.org/10.1111/jfbc.14264>
2. H. Rasouli, M.H. Farzaei, R. Khodarahmi, *Int. J. Food Prop.*, 20(sup2) (2017) 1700-1741. <https://doi.org/10.1080/10942912.2017.1338771>
3. C.G. Fraga, K.D. Croft, D.O. Kennedy, F.A. Tomás-Barberán, *Food Funct.*, 10(2) (2019) 514-528. <https://doi.org/10.1039/C8FO02435G>
4. G. Grosso, *Nutrients*, 10(8) (2018) 1087. <https://doi.org/10.3390/nu10081087>
5. N.B. Rathod, S.M. Nikoo, F. Özogul, J.M. Regenstein, S.N. El, *Plants*, 12(6) (2023) 1217. <https://doi.org/10.3390/plants12061217>
6. S. Ferré, *J. Caffeine Res.*, 3(2) (2013) 57-58. <https://doi.org/10.1089/jcr.2013.0015>
7. V.S. Reddy, H.A. Al-Rashed, S.S. Al-Rawi, R.S. Al-Kharusi, *Eur. J. Med. Chem. Rep.*, 10 (2024) 100138. <https://doi.org/10.1016/j.ejmcr.2023.100138>
8. R. Abalo, *Nutrients*, 13(9) (2021) 2942. <https://doi.org/10.3390/nu13092942>
9. A. Saimaiti, Y. Zhou, J. Li, R. Gan, *Crit. Rev. Food Sci. Nutr.*, 63(29) (2023) 9648-9666. <https://doi.org/10.1080/10408398.2022.2074362>
10. R.C. Emadi, F. Kamangar, *Nutrients*, 17(15) (2025) 2558. <https://doi.org/10.3390/nu17152558>
11. G. Beauchamp, A. Amaducci, M. Cook, *Clin. Pediatr. Emerg. Med.*, 18(3) (2017) 197-202. <https://doi.org/10.1016/j.cpem.2017.07.004>
12. Q. Adeleye, O. Onyeaka, B.A. Enebeli, O. Onigbinde, *Ann. Afr. Med.*, 22(3) (2023) 392-394. https://doi.org/10.4103/aam.aam_150_22
13. I.F. Musgrave, L.S. Akers, R.W. Byard, *Forensic Sci. Med. Pathol.*, 12(3) (2016) 299-303. <https://doi.org/10.1007/s12024-016-9771-7>
14. Q.V. Vuong, J.B. Golding, M.H. Nguyen, P.D. Roach, *Powder Technol.*, 233 (2013) 169-175. <https://doi.org/10.1016/j.powtec.2012.08.026>
15. A. Basaiahgari, V.P.P. Sushma, P. Ijardar, R.L. Gardas, *Fluid Phase Equilib.*, 506 (2020) 112373. <https://doi.org/10.1016/j.fluid.2019.112373>
16. A.M. Ferreira, F.A. Vieira, A.S.S. Pinto, M.G. Freire, *Sustainability*, 13(13) (2021) 7509. <https://doi.org/10.3390/su13137509>
17. N.B. Vuletic, L. Odžak, R. Renata, *Food Res.*, 5 (2021) 325-330. [https://doi.org/10.26656/fr.2017.5\(2\).431](https://doi.org/10.26656/fr.2017.5(2).431)
18. A. Yazdabadi, S.S. Mania, S. Salehifar, *Fluid Phase Equilib.*, 502 (2019) 112287. <https://doi.org/10.1016/j.fluid.2019.112287>
19. S. Ilgaz, I.G. Sat, A. Polat, *J. Food Sci. Technol.*, 55(4) (2018) 1407-1415. <https://doi.org/10.1007/s13197-018-3055-6>
20. I. De Marco, S. Riemma, R. Iannone, *J. Supercrit. Fluids*, 133 (2017) 15-22. <https://doi.org/10.1016/j.supflu.2017.09.020>
21. A.T.E. Santo, R.R.S. Oliveira, J.C.C. Santana, *J. Supercrit. Fluids*, 168 (2021) 105096. <https://doi.org/10.1016/j.supflu.2020.105096>
22. S. Atwi-Ghaddar, C. Vitale, P.S. Garcia, *Molecules*, 28(14) (2023) 5485. <https://doi.org/10.3390/molecules28145485>
23. M. Sökmen, E. Aytaç, S. Alomar, *J. Supercrit. Fluids*, 133 (2017) 203-208. <https://doi.org/10.1016/j.supflu.2017.10.022>
24. T.K. Manios, D. Mattia, M.R. Bird, *Food Bioprod. Process.*, 136 (2022) 14-23. <https://doi.org/10.1016/j.fbp.2022.09.004>
25. T.K. Manios, D. Mattia, M.R. Bird, *Food Bioprod. Process.*, 140 (2023) 1-15. <https://doi.org/10.1016/j.fbp.2023.04.004>
26. T. Zhang, W.H. Tingting, J. Yuqiao, L. Shun, S. Yao, *Food Chem.*, 333 (2020) 127534. <https://doi.org/10.1016/j.foodchem.2020.127534>
27. D. Lai, Y. Zhang, Y. Wang, W. Li, X. Sun, *J. Food Sci.*, 90 (2025) 1-12. <https://doi.org/10.1111/1750-3841.17182>
28. M.L. Mignoni, L.R. Radtke, C. Machado, *Appl. Clay Sci.*, 41(1) (2008) 99-104. <https://doi.org/10.1016/j.clay.2007.09.008>
29. K.C. Willson, M.N. Clifford, *Tea: Cultivation to consumption*, Springer Netherlands, Dordrecht (1992).
30. ISO 14502-1, *Determination of Substances Characteristic of Green and Black Tea-Part 1*, ISO, Geneva (2005).
31. ISO 10727, *Tea and instant tea in solid form — Determination of caffeine content*, ISO, Geneva (2002).
32. W. Plazinski, W. Rudzinski, A. Plazinska, *Adv. Colloid Interface Sci.*, 152(1) (2009) 2-13. <https://doi.org/10.1016/j.cis.2009.09.007>
33. Z.B. Dong, Y.R. Liang, J.L. Lu, H.L. Zheng, *J. Agric. Food Chem.*, 59(8) (2011) 4238-4247. <https://doi.org/10.1021/jf104863f>
34. C.E. Harland, *Ion Exchange: Theory and Practice*, Royal Society of Chemistry, London (1994).
35. A. Proctor, J.F. Toro-Vazquez, *J. Am. Oil Chem. Soc.*, 73(12) (1996) 1627-1633. <https://doi.org/10.1007/BF02517962>
36. H.L. Tan, H.W. Lim, C.P. Leo, *Heliyon*, 9(2) (2023) e12638. <https://doi.org/10.1016/j.heliyon.2023.e12638>
37. M. Cabrera, G. Galli, M.S. Paszkiewicz, *Molecules*, 26(12) (2021) 3485. <https://doi.org/10.3390/molecules26123485>
38. B. Kralj, J. Ščančar, R. Milačič, *Anal. Bioanal. Chem.*, 383(3) (2005) 467-475. <https://doi.org/10.1007/s00216-005-0010-0>
39. R. Street, G. Szakova, O. Drabek, J. Miholova, *Food Chem.*, 104(4) (2007) 1662-1669. <https://doi.org/10.1016/j.foodchem.2007.03.012>

<https://doi.org/10.62239/jca.2026.005>

40. Z. Fu, S. Wang, Y. Zhang, G. Li, *Food Chem.*, 430 (2024) 137000. <https://doi.org/10.1016/j.foodchem.2023.137000>
41. M. Atak, E.Y.K. Derya, Ç. Muhammet, *Appl. Food Res.*, 4(2) (2024) 100626. <https://doi.org/10.1016/j.afres.2024.100626>
42. J.A. Quintero-Jaramillo, J.I. Carrero-Mantilla, N.R. Sanabria-González, *Sci. World J.*, 2021 (2021) 9998924. <https://doi.org/10.1155/2021/9998924>
43. H. Bahrami, M. Tabrizchi, H. Farrokhpour, *Chem. Phys.*, 415 (2013) 222-227. <https://doi.org/10.1016/j.chemphys.2013.01.008>
44. K. Muraoka, W. Chaikittisilp, T. Okubo, *J. Am. Chem. Soc.*, 138(19) (2016) 6184-6193. <https://doi.org/10.1021/jacs.6b01458>
45. N.S. Dionisiou, T. Matsi, *Environmental Materials and Waste*, Academic Press, New York (2016) 591-606.
46. A.M. Ziyath, M.S. Chong, J.W. Ng, *J. Water Resour. Prot.*, 3 (2011) 758-767. <https://doi.org/10.4236/jwarp.2011.311086>
47. M. Hassnain, *Growth of Mordenite Nanocrystals Sans Seed Addition*, University Press, Oxford (2017).
48. S.A.L. Bachmann, T. Calvete, L.A. Féris, *Sci. Total Environ.*, 767 (2021) 144229. <https://doi.org/10.1016/j.scitotenv.2020.144229>
49. M. Fakioğlu, Y. Kalpaklı, *RSC Adv.*, 12(41) (2022) 26504-26513. <https://doi.org/10.1039/D2RA04664B>
50. B. Cantor, *The Equations of Materials*, Oxford University Press, Oxford (2020).
51. A. Adaileh, S. Al-Qura'n, M. Al-Rawajfeh, *Sci. Rep.*, 15(1) (2025) 22250. <https://doi.org/10.1038/s41598-025-22250-w>
52. A.O. Dada, A.A. Inyinbor, J.O. Bello, *Proc. 2024 Int. Conf. Sci. Eng. Bus. Sustain. Dev. Goals, IEEE* (2024) 112-118.
53. D. Robati, *J. Nanostructure Chem.*, 3(1) (2013) 55. <https://doi.org/10.1186/2193-8865-3-55>
54. Z.L. Yaneva, M.S. Staleva, N.V. Georgieva, *Eur. J. Chem.*, 6(2) (2015) 169-173. <https://doi.org/10.5155/eurjchem.6.2.169-173.1206>
55. E. Bulut, M. Özacar, İ.A. Şengil, *Microporous Mesoporous Mater.*, 115(3) (2008) 234-246. <https://doi.org/10.1016/j.micromeso.2008.01.039>
56. K. Jermjun, S. Praserttham, P. Praserttham, *Molecules*, 28(16) (2023) 6019. <https://doi.org/10.3390/molecules28166019>
57. L. Damjanović, V. Rakić, V. Radmilović, *J. Hazard. Mater.*, 184(1) (2010) 477-484. <https://doi.org/10.1016/j.jhazmat.2010.08.059>
58. M.A. Klunk, M.P.A. Wanderley, S.M.O. Silva, *Chem. Pap.*, 74(8) (2020) 2481-2489. <https://doi.org/10.1007/s11696-020-01089-w>
59. F. Chen, X.B. Fan, L.Y. Zhang, J.P. Zhao, *Chem. Eng. Sci.*, 263 (2022) 118110. <https://doi.org/10.1016/j.ces.2022.118110>
60. T. Montanari, M. Bevilacqua, G. Busca, *Appl. Catal. A: Gen.*, 307(1) (2006) 21-29. <https://doi.org/10.1016/j.apcata.2006.03.003>
61. F. Pendolino, *Self-assembly of molecules on nanostructured graphene*, Springer, Berlin (2014).
62. L. Capasso, V. Capasso, G.S. Di Giacomo, *Molecules*, 30(3) (2025) 654. <https://doi.org/10.3390/molecules30030654>